

Mass-number dependence of the forward-angle cross section for pion single-charge-exchange reactions

N. Nose-Togawa,¹ T. Mizushima,² S. Hirenzaki,² and K. Kume²

¹Research Center for Nuclear Physics, Osaka University, Ibaraki 567-0047, Japan

²Department of Physics, Nara Women's University, Nara 630-8506, Japan

(Received 29 January 2003; published 17 March 2004)

The mass-number dependences of the high-energy pion single-charge-exchange reactions are studied under the distorted-wave impulse approximation. The observed forward-angle cross sections are approximately proportional to $(N-Z) \times A^{-\alpha(E)}$ for the isobaric-analog transition and the overall feature is explained in the present calculation. The coefficient $\alpha(E)$ is shown to be strongly dependent on the imaginary part of the optical potential. The observed monotonic decrease of the coefficient $\alpha(E)$ with respect to the incident energy is reproduced but the absolute values of $\alpha(E)$ are smaller than those of experiment. It is also shown that the coefficient $\alpha(E)$ is considerably influenced by the rms radii of the isovector density of the target nuclei.

DOI: 10.1103/PhysRevC.69.034609

PACS number(s): 25.80.Gn, 24.10.Ht, 24.50.+g, 21.60.Jz

I. INTRODUCTION

Pion-nucleus single-charge-exchange (SCX) reactions have been studied from low-energy to high-energy regions [1–9]. Around the Δ -resonance region, measured reaction strength for $^{13}\text{C}(\pi^+, \pi^0)$ has moderate peak structure with respect to the incident pion energy, while the theoretical values exhibit a deep minima around the Δ resonance due to the strong absorption. Despite the theoretical attempts to take into account the medium effects for Δ isobar, this discrepancy still remains [10]. At higher-energy region, the theoretical forward-angle cross sections for the SCX reaction (π^+, π^0) overestimate the experimental values by about a factor 2–3 for ^{14}C [11]. Possible correction coming from the nuclear medium-polarization effect is discussed under the local density approximation [12]. The core-polarization effects for the SCX reaction cross section and the asymmetry are also calculated for ^{13}C and ^{15}N at high-energy region [13]. These works are concerned with the SCX reaction on a specific nucleus. Both the reaction mechanism and the nuclear structure are involved and this complicates the problem. For this reason, it is advantageous to study the case of spinless target nuclei leading to the isobaric-analog state (IAS) since, if we assume the impulse approximation, relevant transition density is the neutron and the proton density difference. The ambiguity coming from the nuclear structure can be minimized.

Observed forward cross sections for the spinless target nuclei leading to IAS exhibit a clear mass-number dependence (A dependence) approximately expressed as $(d\sigma/d\Omega)_{\theta=0^\circ} \propto (N-Z) \times A^{-\alpha(E)}$ [14–16]. The coefficient $\alpha(E)$ monotonically and slowly decreases with the increase of the incident energy from $\alpha(E)=1.40 \pm 0.06$ at 100 MeV to $\alpha(E)=0.82 \pm 0.10$ at 500 MeV. Johnson employed the eikonal approximation and has shown that, in the limit of strong surface absorption, $\alpha(E)=\frac{4}{3}$ [17]. The experimental value at 100 and 165 MeV is close to this limit while decreases monotonically at higher energies. It is argued that the decrease of $\alpha(E)$ with the increase of the incident energy is a consequence of increased volume scattering [16] and it is

interesting to see whether these features could be explained with the conventional distorted-wave impulse approximation (DWIA) calculation.

In the present paper, we examined the mass-number dependence of the SCX reaction for spinless nuclei leading to IAS. If we adopt the plane-wave impulse approximation, forward-angle cross section divided by $N-Z$ is constant with respect to the mass number A [i.e., $\alpha(E)=0$]. Thus, the observed strong A dependence is expected primarily due to the distortion effects. We have carried out the conventional distorted-wave calculation using the isovector nuclear density given by the relativistic Hartree approximation [18]. We show that it reproduces the $A^{-\alpha(E)}$ dependence of the forward-angle cross sections. The monotonic decrease of the coefficient $\alpha(E)$ with the increase of the incident energy is predicted but the theoretical values of $\alpha(E)$ are smaller than those of experiment. We examined the various dependences of the coefficient $\alpha(E)$ on the theoretical inputs. The $\alpha(E)$ is shown to be strongly sensitive to the imaginary part of the optical potential but is quite insensitive to the real part. The nuclear size effects for $\alpha(E)$ are also examined.

In Sec. II, we briefly describe the model and the formula adopted in the present calculation. The results are shown and are discussed in Sec. III. We summarize the results in Sec. IV.

II. FORMULATION

For spinless nuclei, the observed forward-angle (π^+, π^0) cross section is approximately proportional to $N-Z$ times the inverse power $\alpha(E)$ of the mass number A of the target nuclei,

$$\left(\frac{d\sigma}{d\Omega}\right)_{\theta=0^\circ} \propto (N-Z) \times A^{-\alpha(E)}. \quad (1)$$

We can easily show that the plane-wave impulse approximation leads to $\alpha(E)=0$,

$$\left(\frac{d\sigma}{d\Omega}\right)_{\theta=0^\circ} \propto (N-Z). \quad (2)$$

This can be shown as follows. The transition amplitude is written under the impulse approximation as

$$T_{fi} \sim \int \chi_f^*(\mathbf{r}) \langle \Phi_f | \sum_{j=1}^A t \delta(\mathbf{r} - \mathbf{r}_j) \boldsymbol{\pi}(j) \cdot \mathbf{I} | \Phi_i \rangle \chi_i(\mathbf{r}) d\mathbf{r}. \quad (3)$$

We consider the case of IAS transition $(T, T_z) \rightarrow (T, T_z + 1)$ on spinless nuclei. Assuming the plane-wave approximation, the forward reaction amplitude can be written as

$$T_{fi} \sim \int \langle TT_z + 1 | \sum_{j=1}^A t \boldsymbol{\pi}(j) \cdot \mathbf{I} | TT_z \rangle \quad (4)$$

$$= t \langle TT_z + 1 | \sqrt{2T_+} | TT_z \rangle \quad (5)$$

$$= 2\sqrt{2}t \sqrt{(T - T_z)(T + T_z + 1)}. \quad (6)$$

In the present case, $T = -T_z$ and $T_z = (Z - N)/2$, and hence

$$T_{fi} \propto \sqrt{N - Z}. \quad (7)$$

Then the forward-angle cross section $(d\sigma/d\Omega)_{\theta=0^\circ}$ is proportional to $N - Z$. Thus, the observed strong mass-number dependence is considered to come primarily from the pion distortion effects. Johnson has shown under the eikonal approximation that the coefficient $\alpha(E) = \frac{4}{3}$ for the strong absorption limit [17]. The observed A dependence is close to this value around the Δ resonance region but decreases monotonically at higher-energy regions. We have carried out calculations under the distorted-wave impulse approximation to see to what extent the observed mass-number dependence and its energy dependence are reproduced.

First, we describe the theoretical model used in the present work. The distorted-wave impulse approximation in momentum space is adopted to calculate the SCX amplitude. The pion-nucleon scattering amplitude of the spin-nonflip part is decomposed into its partial-wave components as

$$t(\mathbf{k}', \mathbf{k}; \omega) = \sum_{\lambda} t_{\lambda}(k_0) P_{\lambda}(\cos \theta), \quad (8)$$

where k_0 is the on-shell momentum corresponding to the pion energy ω . We adopt the pion-nucleon phase shifts taken from the database SAID [19] and retain the partial waves up to $\lambda=6$, and assume the off-shell extrapolation of the pion-nucleon amplitude

$$t_{\lambda}(k_0) \rightarrow t_{\lambda}(k, k'; \omega) = t_{\lambda}(k_0) g_{\lambda}(k) g_{\lambda}(k') \quad (9)$$

with the Gaussian-type form factor

$$g_{\lambda}(k) = \left(\frac{k}{k_0}\right)^{\lambda} \exp\left[-\left(\frac{k - k_0}{\Lambda}\right)^2\right]. \quad (10)$$

Under the distorted-wave impulse approximation, the transition amplitude for the SCX reaction on spinless nucleus is expressed as

$$\begin{aligned} T_{fi} = & -\frac{1}{\sqrt{T}} \sum_{\ell} (2\ell + 1) P_{\ell}(\cos \theta) \sum_{\lambda, \ell_1} \frac{2\ell_1 + 1}{2\lambda + 1} t_{\lambda}(k_0) (\ell \ell_1 0 0 | \lambda 0)^2 \\ & \times \int r^2 dr \left[\int j_{\ell_1}(kr) \phi_{\ell}^{(f)}(k) g_{\lambda}(k) k^2 dk \right]^* \\ & \times \left[\int j_{\ell_1}(k'r) \phi_{\ell}^{(i)}(k') g_{\lambda}(k') k'^2 dk' \right] \rho_T(r), \end{aligned} \quad (11)$$

where $\phi_{\ell}^{(i)}(k)$ and $\phi_{\ell}^{(f)}(k)$ are the initial and the final pion radial wave functions in momentum space. $\rho_T(r)$ is the transition density leading to IAS and is given as

$$\rho_T(r) = \langle J = 0 TT_z + 1 | \sum_j \tau_+(j) \delta(\mathbf{r} - \mathbf{r}_j) | J = 0 TT_z \rangle. \quad (12)$$

The isovector density of the spinless nucleus is defined as

$$\delta\rho(r) = \rho_p(r) - \rho_n(r) \quad (13)$$

$$= \langle J = 0 TT_z | \sum_j \tau_0(j) \delta(\mathbf{r} - \mathbf{r}_j) | J = 0 TT_z \rangle, \quad (14)$$

which is normalized to

$$\int \delta\rho(r) d\mathbf{r} = Z - N, \quad (15)$$

and is related to $\rho_T(r)$ as

$$\rho_T(r) = -\frac{\sqrt{(T - T_z)(T + T_z + 1)}}{\sqrt{2T_z}} \delta\rho(r). \quad (16)$$

Then, we can calculate the SCX transition density from the isovector density of the target nucleus.

The pion distorted waves are generated by the first-order pion-nucleon optical potential as

$$\langle \mathbf{k}' | V_{\text{opt}} | \mathbf{k} \rangle \simeq \frac{A - 1}{A} \rho(\mathbf{q}) \langle \mathbf{k}' \mathbf{p}' | t | \mathbf{k} \mathbf{p} \rangle, \quad (17)$$

where $\mathbf{q} = \mathbf{k}' - \mathbf{k}$. \mathbf{k} and \mathbf{p} are the pion and the nucleon momenta in the pion-nucleon center-of-mass system and $\rho(\mathbf{q})$ the nuclear density. By neglecting the nucleon Fermi motion in the nucleus, we fix the nucleon momenta to be $\mathbf{p} = -\mathbf{k}/A$ and $\mathbf{p}' = -\mathbf{k}'/A$, and the optical potential can be expressed as

$$\langle \mathbf{k}' | V_{\text{opt}} | \mathbf{k} \rangle \simeq \frac{A - 1}{A} \rho(\mathbf{q}) \Gamma \langle \boldsymbol{\kappa}' | t | \boldsymbol{\kappa} \rangle, \quad (18)$$

where $\boldsymbol{\kappa}$ and $\boldsymbol{\kappa}'$ are the pion momenta in the pion-nucleon center-of-mass frame and the kinematical transformation factor Γ is given by

$$\Gamma = \left[\frac{\omega(\boldsymbol{\kappa}) \omega(\boldsymbol{\kappa}') E(\boldsymbol{\kappa}) E(\boldsymbol{\kappa}')}{\omega(k) \omega(k') E\left(\frac{k}{A}\right) E\left(\frac{k'}{A}\right)} \right]^{1/2}, \quad (19)$$

with the pion and the nucleon energies

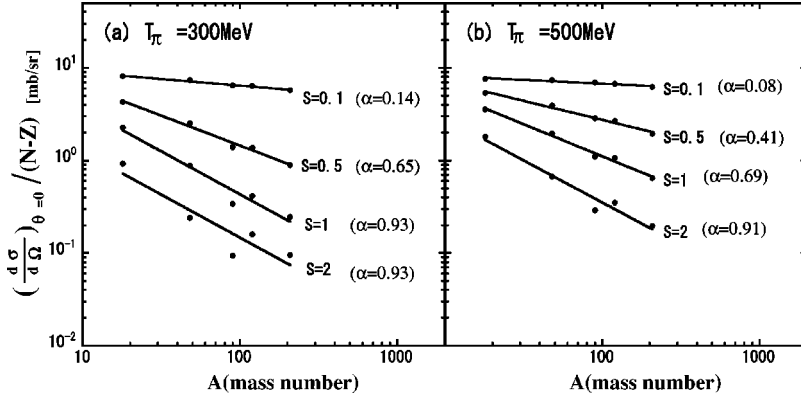


FIG. 1. The dots are the theoretical forward-angle cross section for the SCX cross section leading to IAS divided by $N-Z$ for ^{18}O , ^{48}Ca , ^{90}Zr , ^{120}Sn , and ^{208}Pb at (a) $T_\pi=300$ MeV and (b) $T_\pi=500$ MeV. The calculations are done by multiplying the scale factor S to the pion-nucleus optical potential. We have varied the factor S from 0.1 to 2. The solid lines are the fit to these theoretical values assuming the dependence $A^{-\alpha(E)}$. The calculated coefficients $\alpha(E)$ are shown in the parentheses.

$$\omega(\kappa) = \sqrt{\kappa^2 + \mu^2} \quad (20)$$

and

$$E(\kappa) = \sqrt{\kappa^2 + M^2}. \quad (21)$$

In the above equation, we neglected the angle transformation from pion-nucleon to pion-nucleus center-of-mass frames. The partial-wave decomposition of the optical potential is straightforward and we obtain

$$V_\ell^{\text{opt}} = \frac{4\pi}{2\ell+1} \sum_{\lambda, \ell'} t_\lambda(k, k'; \omega) (\lambda \ell' 00 | \ell 0)^2 \rho_{\ell'}(k, k'), \quad (22)$$

where $\rho_{\ell'}(k, k')$ is the coefficient of the multipole expansion of the nuclear density $\rho(r)$

$$\int e^{-ik'\cdot r} \rho(r) e^{ik\cdot r} d\mathbf{r} = \sum_\ell \rho_\ell(k, k') P_\ell(\cos \theta). \quad (23)$$

The pion-nucleus distorted waves are calculated by the Klein-Gordon equation in momentum space

$$(k_0^2 - k^2) \phi_\ell(k) = 2\omega \int V_\ell^{\text{opt}}(k, k') \phi_\ell(k') k'^2 dk'. \quad (24)$$

The above equation is discretized and the conventional matrix inversion method is used to solve the integral equation. For the cutoff mass in Eq. (10), we take $\Lambda=0.8$ GeV which was used in the analysis of the pion-nucleon elastic scattering [20].

III. RESULTS

We show the results of our calculation for SCX cross sections leading to the isobaric analog states for several spinless nuclei. The nuclear isovector densities, $\delta\rho(r) = \rho_p - \rho_n$, are calculated with the relativistic Hartree model [18]. The calculations are done in momentum space for some typical nuclei ^{18}O , ^{48}Ca , ^{90}Zr , ^{120}Sn , and ^{208}Pb . The nuclear density in the pion-nucleus optical potential is calculated with the harmonic-oscillator density for ^{18}O and the Woods-Saxon form for heavier nuclei. The density parameters are taken from Ref. [21] and the radius parameters are scaled from the nearby nuclei by assuming the $A^{1/3}$ dependence.

First, we calculate the forward-angle cross section by varying the strength of the pion-nucleus optical potential to

see the distortion effects. We have introduced a single free parameter S and multiplied it to the pion-nucleus optical potential

$$V_{\text{opt}} \rightarrow S \times V_{\text{opt}}. \quad (25)$$

The results are shown in Fig. 1 as the dots at the pion incident energies $T_\pi=300$ and 500 MeV. As seen, the calculated forward-angle cross sections decrease with the increase of the parameter S and this shows that the pion distortion significantly influences the forward-angle cross section and the distortion effect is stronger for heavier nuclei which leads to the A dependence of the forward cross section. These features are almost the same for both the incident energies $T_\pi=300$ and 500 MeV. We assumed the dependence $(d\sigma/d\Omega)_{\theta=0} \propto (N-Z) \times A^{-\alpha(E)}$ and obtained the coefficient $\alpha(E)$ by fitting to the theoretical values of the cross section. The results are shown in the figure. Obviously, $\alpha(E) \sim 0$ for weak distortion $S \sim 0$. Next, we have multiplied factors S_R and S_I separately to the real and the imaginary parts of the pion-nucleus optical potential as

$$V_{\text{opt}} \rightarrow S_R \times \text{Re}(V_{\text{opt}}) + iS_I \times \text{Im}(V_{\text{opt}}), \quad (26)$$

and have varied S_R and S_I ($0 \leq S_R, S_I \leq 1$). The results are shown in Figs. 2 and 3. It is interesting to see that the forward-angle cross sections are quite *insensitive* to the real part of the pion-nucleus optical potential as seen in Fig. 2. For incident pion energy $T_\pi=300$ MeV, the cross sections slightly decrease with the increase of S_R but, at the incident energy $T_\pi=500$ MeV, the cross sections are almost the same for various choices of S_R . On the other hand, the forward-angle cross sections are strongly *sensitive* to the imaginary part of the pion-nucleus optical potential as seen in Fig. 3. At incident energy $T_\pi=300$ MeV, the absolute value of the cross sections decreases with the increase of S_I while the coefficient $\alpha(E)$ is only slightly affected. At $T_\pi=300$ MeV, $\alpha(E)=0.86$ even for small, $S_I=0.1$ while, at $T_\pi=500$ MeV, the slope coefficient is very small, $\alpha(E)=0.11$ for $S_I=0.1$. As shown, the SCX forward-angle cross sections are strongly dependent on the imaginary part of the optical potential but the detailed features depend on the pion incident energies.

The theoretical values are compared with the experimental data from $T_\pi=100$ to 500 MeV in Fig. 4. In this figure,

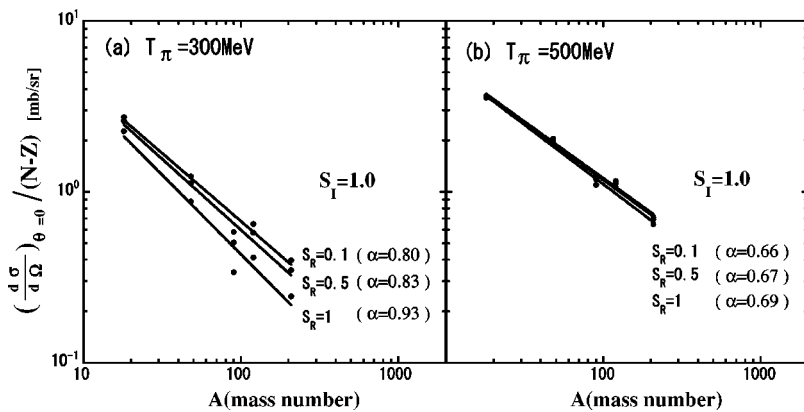


FIG. 2. The dots are the theoretical forward-angle cross section for the SCX cross section divided by $N-Z$ for ^{18}O , ^{48}Ca , ^{90}Zr , ^{120}Sn , and ^{208}Pb at (a) $T_\pi=300$ MeV and (b) $T_\pi=500$ MeV. The calculations are done by multiplying the factor S_R to the real part of the pion-nucleus optical potential while the imaginary part is unaltered ($S_I=1$). The solid lines are the fit to these theoretical values assuming the dependences $A^{-\alpha(E)}$. The calculated coefficients $\alpha(E)$ are shown in the parentheses.

the open circles represent the theoretical results with the nuclear isovector densities calculated with the relativistic Hartree model. The fitted values $\alpha(E)$ are also shown in the figure. The experimental data are also shown with the coefficients $\alpha(E)$. The calculated coefficients $\alpha(E)$ monotonically decrease with the increase of the incident energies in conformity with the experimental data. However, the absolute values of the theoretical cross sections are larger by about a factor 2–3 at high energies $T_\pi=300$ –500 MeV.

In Ref. [16], Rokni *et al.* have shown that the Glauber amplitude overestimates the experimental cross section. They introduced the two-body absorption term phenomenologically with a single energy-independent free parameter c which is adjusted to fit the experimental data. They could explain the experiment fairly well and thus attributed the discrepancy between the Glauber calculation and experiment to the pion absorption effects. Both the pion distortion and the absorption effects reduce the small impact-parameter components and, if we take the constant absorption coefficient c with respect to the pion energy, the pion absorption effect is pronounced at high energies where distortion effect is weaker. Thus, in Ref. [16], the reduction of the cross section due to the pion absorption is fairly large at higher energies. After that, Oset and Strottman [22] made detailed theoretical calculation of the pion absorption effects and have shown that there is a strong energy dependence for the absorption parameter c , which was not considered in Ref. [16]: the two-body absorption coefficient c decreases by about a factor 15 from $T_\pi=200$ to 600 MeV. Then the reduction of the cross section due to the pion absorption is shown to be about 10% at $T_\pi=300$ MeV and only about 5% at T_π

=550 MeV. Thus, the discrepancy of the absolute value of the forward cross section between theory and experiment still remains after considering the pion absorption effects. Oset *et al.* claimed that this discrepancy can be explained by introducing the medium-polarization effect [12]. We reexamined the pion absorption effect for the SCX cross section around the resonance where the coordinate-space calculation is possible, and have checked that it affects the forward-angle SCX cross section by only about 10%. Our results based on the optical potential approach are close to those of the Glauber approximation without pion absorption in Ref. [22]. For the detailed comparison with the experiment, we should apply more sophisticated nuclear models and also examine the medium-polarization effect. In the present work, we applied a somewhat crude model to see the overall trends of the A dependence for the forward SCX cross section.

In the present calculation, we assumed the pion-nucleus optical potential of the $t\rho$ type. As is known, such a first-order optical potential slightly underestimates the experimental value of the elastic scattering cross section at forward direction and considerably underestimates around the second peak [13,20]. Previously, we have adjusted the potential parameters to fit the elastic scattering cross section and used the best-fit potential to calculate the SCX cross section [13]. As shown, the theoretical results of the SCX cross section with the first-order potential and the best-fit potential are quite similar and the difference is only 4% at $T_\pi=800$ MeV for ^{13}C [13]. Thus, we have applied the $t\rho$ potential throughout.

Roughly speaking, the DWIA amplitude of the SCX cross section is the overlap of the nuclear isovector density $\delta\rho$ and the pion wave function. Thus, we expect that the absolute values of the cross sections are sensitive to the rms radii of

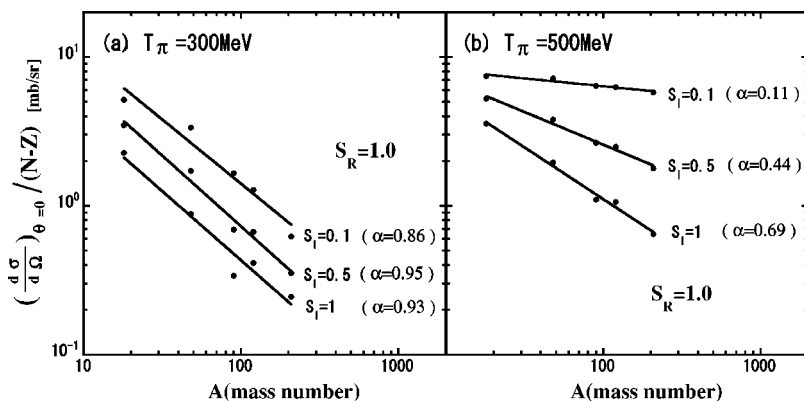


FIG. 3. The same as in Fig. 2, but by multiplying the scale factor to the imaginary part of the pion-nucleus optical potential while the real part is unaltered ($S_R=1$).

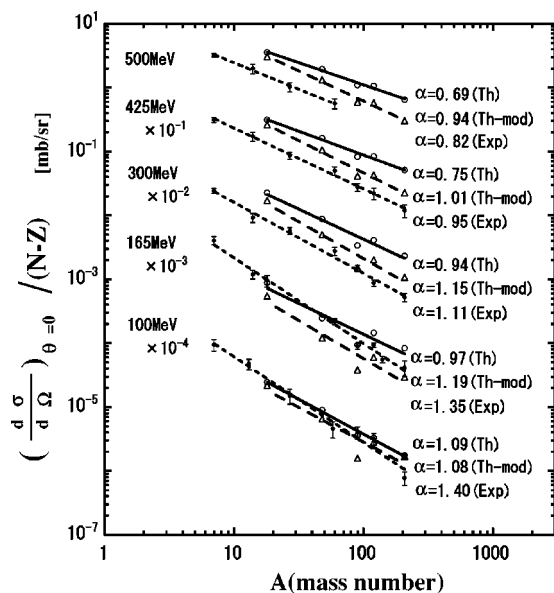


FIG. 4. The forward-angle SCX cross section leading to the IAS divided by $N-Z$ for ^{18}O , ^{48}Ca , ^{90}Zr , ^{120}Sn , and ^{208}Pb at various pion incident energies. The open circles represent the DWIA calculations with the transition density by relativistic Hartree model (Th). The open triangles are with the modified transition density described in the text (Th-mod). The experimental data are taken from Refs. [14–16]. The solid, long-dashed, and short-dashed lines are the fits to these values by assuming the mass-number dependence $A^{-\alpha(E)}$.

the isoscalar and the isovector density. The input parameters of the relativistic Hartree model were adjusted to reproduce the experimental rms radii of the nuclear charge density [18]. The relativistic Hartree model gives the mass-number dependence of the rms radii of the isovector density approximately as $r_0 A^\beta$ with $r_0=1.73$ fm and $\beta=0.237$ while $r_0=1.16$ fm and $\beta=0.293$ for the isoscalar density. In the present calculation, we have calculated the pion distorted waves in momentum space. Thus, it is quite difficult to calculate the high-momentum matrix elements $\rho_{\ell'}(k, k')$ in Eq. (22) with the isoscalar densities by the relativistic Hartree model. Instead, we have adopted the isoscalar nuclear densities from the work of Ref. [21]. We have evaluated the nuclear radius parameter by assuming the mass-number dependence $A^{1/3}$ from the nearby nuclei: the nuclear radius of ^{48}Ca is obtained by extrapolating from that of ^{40}Ca , etc. Strictly, this is not a consistent procedure. We should use the same nuclear model to predict both the isoscalar and the isovector densities. Since the DWIA amplitude of the SCX cross section is the overlap of the nuclear isovector density $\delta\rho$ and the pion wave function, we expect that the absolute values of the cross sections are sensitive to the relative size of the isoscalar and isovector densities. To see this dependence, we have checked the sensitivity of the cross section to the nuclear size. We simply scaled the isovector density in an *ad hoc* way so as to give $r_0=1.73$ fm and $\beta=0.2$ for the rms radii of the isovector density. The results are shown in Fig. 4 as the open triangles with the long dashed lines denoted as (Th-mod). The narrower isovector densities give smaller overlap of the pion and the nucleon wave functions resulting in the

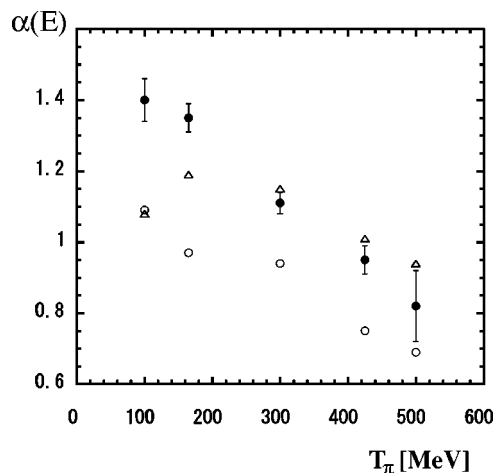


FIG. 5. The energy dependence of the coefficient $\alpha(E)$. The open circles are the results of the DWIA calculation with the isovector density by relativistic Hartree model (Th). The open triangles are the results of DWIA calculation with the modified transition density described in the text (Th-mod). The experimental data are taken from Refs. [14–16].

smaller cross sections. As seen, the size effects are appreciably large and are dependent on the pion energy. For the detailed comparison with the experimental data, we need to use more refined nuclear models to calculate the nuclear densities. In the present work, we adopted the relativistic Hartree model to see the overall trends of the A dependence of the cross section.

The energy dependence of the slope coefficient $\alpha(E)$ is shown in Fig. 5. The open circles are the results of the DWIA calculation with the isovector density by the relativistic Hartree model. In Fig. 5, the open triangles are the results of DWIA calculation with the modified isovector densities described above. For this modification of the isovector densities, the absolute values of the cross section decrease at high-energy region, while are almost the same for $T_\pi=100$ MeV as seen in Fig. 4. The coefficients $\alpha(E)$ are close to the experiment at higher energies but are smaller at low energies. For more detailed comparison with the experiment, more elaborate treatment of the nuclear densities and also the inclusion of the medium-polarization effects should be necessary.

IV. CONCLUSION

Observed forward-angle cross sections for the spinless nuclei leading to IAS exhibit a clear mass-number dependence approximately expressed as $(d\sigma/d\Omega)_{\theta=0} \propto (N-Z) \times A^{-\alpha(E)}$ [14–16]. The coefficient $\alpha(E)$ monotonically and slowly decreases with the increase of the incident energy. Johnson employed the eikonal approximation and has shown that in the limit of strong surface absorption $\alpha(E)=\frac{4}{3}$ [17]. The experimental value at $T_\pi=100$ and 165 MeV is close to this limit while decreases monotonically at higher energies. In the present paper, we examined the mass-number dependence of the SCX reaction for spinless nuclei leading to the isobaric analog states. The plane-wave impulse approxima-

tion predicts that the forward-angle cross section divided by $N-Z$ is constant with respect to the mass number [i.e., $\alpha(E)=0$]. Thus, the observed strong A dependence is expected primarily due to the distortion effects. We have carried out the conventional distorted-wave calculation using the isovector nuclear density by the relativistic Hartree model [18]. In the present work, we assumed the distorted-wave impulse approximation with the $t\rho$ -type pion-nucleus optical potential. Previously, we have shown that the best-fit potential to the elastic scattering gives the SCX cross section only a few percent different from those of the first-order potential.

We have shown that the DWIA calculation reproduces the overall trends of the dependence $A^{-\alpha(E)}$ of the forward-angle cross sections. The monotonic decrease of the coefficient

$\alpha(E)$ with the increase of the incident energy is also predicted but the theoretical values of $\alpha(E)$ are smaller than those of experiment and also the absolute values of the theoretical cross sections are larger than those of experiment. We examined the various dependences of the coefficient $\alpha(E)$ on the theoretical inputs. The $\alpha(E)$ is strongly *sensitive* to the imaginary part of the optical potential but is rather *insensitive* to the real part. The nuclear size effects for $\alpha(E)$ are also examined and are shown to be fairly large and energy dependent. For the detailed comparison with the experiment, we need to use the more elaborate nuclear models for the nuclear densities and also need to examine the nuclear polarization effects systematically for the absolute value and the A dependence of the forward-angle SCX cross sections.

-
- [1] J. Alster and J. Warszawski, *Phys. Rep.* **52**, 87 (1979).
 [2] A. Doron *et al.*, *Phys. Rev. C* **26**, 189 (1982).
 [3] W. B. Kaufmann and W. R. Gibbs, *Phys. Rev. C* **28**, 1286 (1983).
 [4] L. E. Ussery *et al.*, *Phys. Rev. C* **38**, 2761 (1988).
 [5] J. J. G3rgen *et al.*, *Phys. Rev. Lett.* **66**, 2193 (1991).
 [6] S. S. Kamalov, C. B. Bennhold, and R. Mach, *Phys. Lett. B* **259**, 410 (1991).
 [7] P. B. Siegel and W. R. Gibbs, *Phys. Rev. C* **48**, 1939 (1993).
 [8] P. BydŹovsŹy, R. Mach, and S. S. Kamalov, *Nucl. Phys.* **A574**, 685 (1994).
 [9] N. Nose-Togawa and K. Kume, *Phys. Rev. C* **54**, 432 (1996).
 [10] S. Taniguchi, T. Sato, and H. Ohtsubo, *Prog. Theor. Phys.* **102**, 333 (1999), and references therein.
 [11] G. E. Parndl, D. J. Ernst, and D. R. Giebink, *Phys. Lett. B* **205**, 135 (1988).
 [12] E. Oset, D. Strottman, H. Toki, and J. Navarro, *Phys. Rev. C* **48**, 2395 (1993).
 [13] N. Nose-Togawa and K. Kume, *Phys. Rev. C* **66**, 054603 (2002).
 [14] H. W. Baer *et al.*, *Phys. Rev. Lett.* **45**, 982 (1980).
 [15] U. Sennhauser *et al.*, *Phys. Rev. Lett.* **51**, 1324 (1983).
 [16] S. H. Rokni *et al.*, *Phys. Lett. B* **202**, 35 (1988).
 [17] M. B. Johnson, *Phys. Rev. C* **22**, 192 (1980).
 [18] D. Hirata, H. Toki, T. Watabe, I. Tanihata, and B. V. Carlson, *Phys. Rev. C* **44**, 1467 (1991).
 [19] R. A. Arndt *et al.*, *Phys. Rev. D* **43**, 2131 (1991).
 [20] M. Arima, K. Masutani, and R. Seki, *Phys. Rev. C* **44**, 415 (1991).
 [21] K. Stricker, H. McManus, and J. A. Carr, *Phys. Rev. C* **19**, 929 (1979).
 [22] E. Oset and D. Strottman, *Phys. Rev. C* **42**, 2454 (1990).